PROCEEDINGS OF SPIE

SPIEDigitalLibrary.org/conference-proceedings-of-spie

Piezoelectric cement sensor and impedance analysis for concrete health monitoring

Huang Hsing Pan, Yong-De Wong, Yu-Min Su

Huang Hsing Pan, Yong-De Wong, Yu-Min Su, "Piezoelectric cement sensor and impedance analysis for concrete health monitoring," Proc. SPIE 10971, Nondestructive Characterization and Monitoring of Advanced Materials, Aerospace, Civil Infrastructure, and Transportation XIII, 109710Y (1 April 2019); doi: 10.1117/12.2514306

SPIE.

Event: SPIE Smart Structures + Nondestructive Evaluation, 2019, Denver, Colorado, United States

Piezoelectric Cement Sensor and Impedance Analysis for Concrete Health Monitoring

Huang Hsing Pan*[a], Yong-De Wong[a], Yu-Min Su[a],
[a] Department of Civil Engineering, National Kaohsiung University of Science and Technology, Kaohsiung 80778, Taiwan

ABSTRACT

Piezoelectric cement, instead of PZT (lead zirconate titanate) sensors and smart aggregate, has been developed as a new piezoelectric sensor that particularly applies to monitor concrete structures. Piezoelectric cement is a 0-3 type cement-based piezoelectric composite with 50% PZT for improving the incompatibility of acoustic impedance and volume deformation between conventional piezoelectric sensors and concrete structure. Piezoelectric cement was installed in concrete to monitor the strength development with the age and to detect the damage of concrete by electromechanical impedance technique. The PZT sensor was the counterpart in the experiments. Results indicate that, similar to PZT sensors, piezoelectric cement exhibits the capability of monitoring concrete structures, and the sensitivity of monitoring for piezoelectric cement even better than for the PZT if the piezoelectric cement with suitable piezoelectric strain factor d_{33}. Piezoelectric cement embedded in concrete structures show no resonant frequency in the conductance-frequency spectra that causes to assess the conductance change easily. For the piezoelectric cement with d_{33} = 101 pC/N, the intervals of frequency are 300–660 kHz and 1000–2000 kHz for the strength monitoring and the damage detection, respectively. Broad effective frequency range provides larger RMSD value of conductance.

Keywords: cement sensor, concrete materials, impedance, structural health monitoring

INTRODUCTION

Piezoelectric sensors and actuators as an online monitoring system applied to structural health monitoring (SHM) in civil infrastructures, such as tunnel lining, bridges, road pavement, RC structures and concrete members, have been widely used over two decades [1-8], where PZT sensors and smart aggregates [9] were common used. Instead of conventional piezoelectric ceramics and polymers, cement-based piezoelectric sensors have been developed for structural health monitoring especially in concrete structures to overcome the matching problem of acoustic impedance and deformation with concrete since 2002. Cement-based piezoelectric sensors especially for 1-3 type and 2-2 type have higher piezoelectric properties than 0-3 type, and some 1-3 type and 2-2 type cement-based piezoelectric sensors were applied for traffic monitoring and the damage of concrete [10-12].

*pam@nkust.edu.tw; Tel: +886 7 3814526 ext. 15231; Fax: +886 7 3831371

Nondestructive Characterization and Monitoring of Advanced Materials, Aerospace, Civil Infrastructure, and Transportation XIII, edited by A. L. Gyekenyesi, T.-Y. Yu, H. F. Wu, P. J. Shull, Proc. of SPIE Vol. 10971
109710Y · © 2019 SPIE · CCC code: 0277-786X/19/$18 · doi: 10.1117/12.2514306

For 0-3 type cement-based piezoelectric sensors (piezoelectric cement), many efforts [13-20] to fabricate high piezoelectric properties of piezoelectric cement that can be selected as sensors and actuators are still on-going. Piezoelectric cement via frequency, mechanical-electric response and acoustic emission technology have been proposed applied for SHM [21-26] in concrete structures. However, piezoelectric cement as sensors applied for SHM in conjunction with electromechanical impedance (EMI) technique are seldom reported due to its low piezoelectric properties, where EMI technique is one of monitoring methods for SHM based on electric impedance-frequency spectra variation of piezoelectric sensors [12,27].

In this study, piezoelectric cement as the transducer that embedded in concrete was investigated for monitoring the strength development and detecting the damage of concrete member by using EMI method. Piezoelectric cement (PP sensor) consists of equal PZT and cement by volume, with one was cured at 23℃ and the other at 140℃. Piezoelectric ceramic (PZT sensor) was the counterpart in the experiments. PP and PZT sensors had the same polarization conditions, having 150℃ poling temperature, 1.5 kV/mm poling voltage and 40 min poling time.

2. EXPERIMENTAL PROGRAM

2.1 Piezoelectric specimens

In order to diminish the difference of acoustic impedance and deformation between PZT sensors and concrete, the piezoelectric cement (a 0–3 cement piezoelectric composite) was a two-phase PZT/cement composite with 50 vol.% of PZT ceramic and type I Portland cement equally, where acoustic impedance (ρ_v) of piezoelectric cement was about 10×10^{-6} kg-m^{-2}s^{-1} that close to concrete with $\rho_v = 9.0\times10^{-6}$ kg-m^{-2}s^{-1} [13]. Fresh cement was required with the fineness of 349 m^2/kg. The PZT ceramic was the Ka type provided by Eleceram Technology (Taiwan) with the piezoelectric strain factor d_{33} = 470 pC/N, relative dielectric constant $\varepsilon_r = 2100$ and the density $\rho = 7.9\times10^3$ kg/m^3. The particle size of the PZT ceramic was between the range of 75 and 150 μm.

To prepare the specimen of piezoelectric, PZT particles and cement were uniformly mixed without additional water. Then the mixture was put into a 15-mm-diameter cylindrical steel mold and applied to 80 MPa compression, forming a flaky specimen. Specimens were cured at 90℃ and 100% relative humidity for 24 h to ensure suitable strength. After that, specimens were polished to a 2-mm thickness. Two levers of temperature were defined as A = 23℃ and B = 140℃. Each specimen was heated either to Temperature A or B twice [28] so that two kinds of the specimen were fabricated denoted as PPAA and PPBB. For the specimen of PZT ceramic, the size with 12-mm diameter and 1.8-mm thickness was provided by commercial company. There was no temperature treatment for PZT ceramic

2.2 Polarization and piezoelectric strain factor

For the polarization of the PP and PZT specimens, specimens were placed in 150℃ silicone oil bath and a 1.5 kV/mm poling field was applied for 40 min. After the polarization process was completed, the specimens were measured at controlled condition of 25℃ and 50% relative humidity for 100 days. The piezoelectric strain factor d_{33} was directly measured using a d_{33} piezometer with a dynamic force frequency of 110 Hz, shown in Fig. 1. Each experimental value

shown in the results is an average of three specimens. Results indicated that the d_{33} values of PZT were not sensitive to the age and the value was 399 pC/N. However, the d_{33} values of piezoelectric cement (PPAA and PPBB) depend on the age and will approach to the constant after 70 days, where d_{33} = 55 pC/N for PPAA and d_{33} = 101 pC/N for PPBB. It seems that the PPBB has the higher d_{33} value than PPAA due to temperature treatment. This implies that the piezoelectric cement for PPBB is feasible as piezoelectric sensors, compared with PPAA.

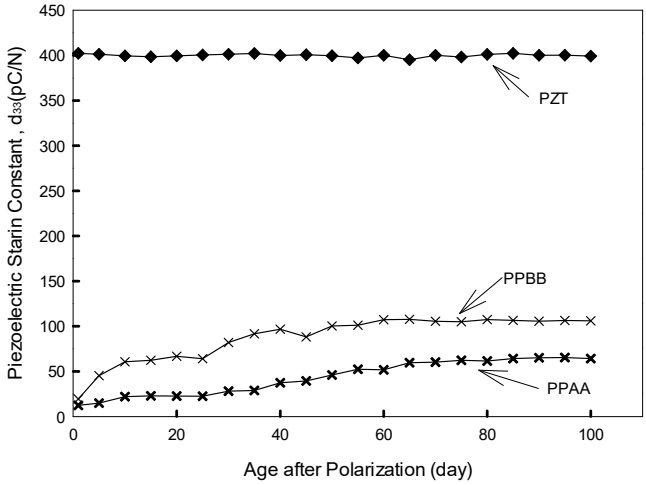

Figure 1. The piezoelectric strain factor of PZT and PP specimens

2.3 Concrete specimens

Two concrete specimens including concrete cylinder and concrete beam were made. Both have the same mixture proportion listed in Table 1. The water-to-binder ratio was 0.58 and the water-reducing admixture with 1% binder was also used. The size of concrete cylinder was Ø100×200 mm, and that of concrete member was 150×150×530 mm.

Table 1. Mixture proportion of concrete

Materials	Cement	Slag	Fly ash	Water	Fine aggregate	Coarse aggregate
kg/m^3	277	55	14	201	860	952

2.4 Piezoelectric sensors set-up

The piezoelectric sensors were tailored by the specimens of PZT, PPAA and PPBB, respectively, as sensing elements and asphalt as packaging material. Because of the age-sensitive d_{33} of PP elements, copper conductive wire was first welded to silver electrode on both surface sides of the PP element at 100 days. Then the packaging material entirely covered the sensing elements and the conductive wires to ensure the insulation ability of the sensors. For the concrete cylinder, piezoelectric sensors were placed in the center of the specimen to monitor the development of the strength, shown in Fig. 2. Meanwhile, piezoelectric sensors were embedded at four positions of the concrete beam shown in Fig. 3 to detect the damage of the beam during the loading, where each piezoelectric sensor was fixed in the center of a carrier (cement plate)

with the size of 50×50×7 mm. A flaw was pre-arranged in the middle of the span to make sure the crack propagation along the depth of middle span.

Figure 2. The piezoelectric sensor was placed in the middle of concrete cylinder

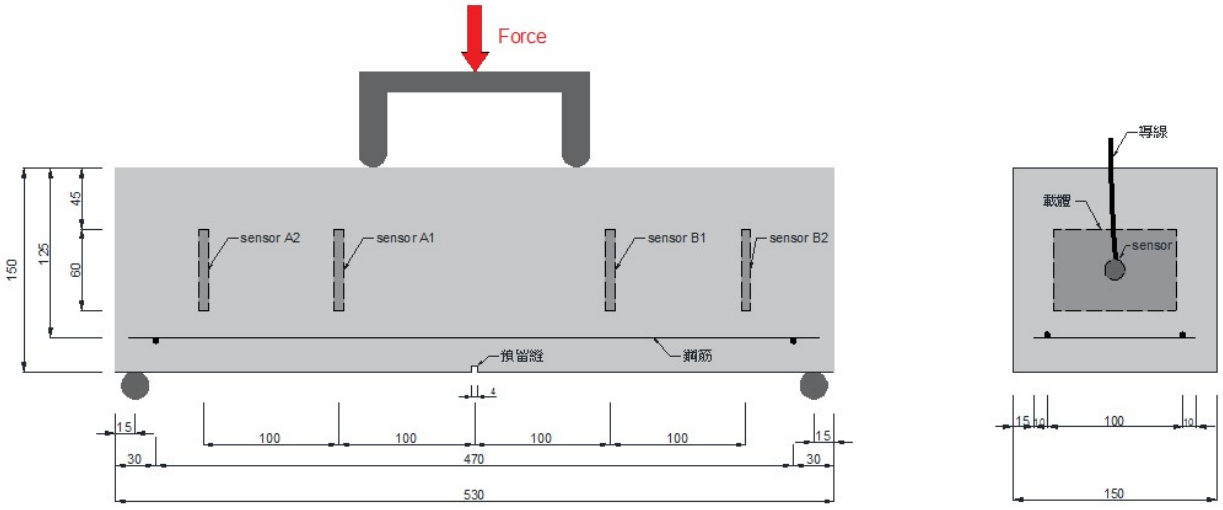

Figure 3. Four piezoelectric sensors (A1、A2、B1 and B2) were embedded in the concrete beam

2.5 Electromechanical impedance measurement

Any change of the mechanical properties in host structure causes changes in the mechanical impedance that induces changes in the electrical impedance of the piezoelectric sensor embedded in structure [29]. From the report by Park *et al* [30], the imaginary part of the electrical admittance (the reciprocal of impedance) is pretty sensitive to the temperature variation than the real part (conductance), that is, the conductance (the reciprocal of resistance) is more preferable for structural health monitoring. Here, impedance analyzer (Wayne Kerr 6520A) was used to acquire the impedance-frequency curve of piezoelectric sensors under the frequency range of 20 – 2000 kHz, and the conductance -frequency curves were used to analyze the strength development of concrete cylinder and the damage of the beam subjected to loading.

3. RESULTS AND DISCUSSION

3.1 Strength monitoring

First, compressive strength of cylinder specimens was tested at the age of 1, 3, 7, 14, 21, 28 and 56 days, respectively. For those cylinder specimens embedded piezoelectric sensors, one measured the impedance-frequency of piezoelectric sensors at the same ages. Fig. 4 shows the conductance signatures of the PZT at 1–56 days corresponding to the day of compressive strength tests, and serval resonant peaks were observed. However, there is only the range of 320-380 kHz (zone B) having the tendency of conductance reduction as the curing day increases shown in Fig. 5, where the monitoring age is from day 1 (D1) to days56 (D56). In order to link up the strength development of concrete corresponding to conductance variations, the root-mean-square-deviation (RMSD) was employed [30]. Fig.6 is the comparison between compressive strength and the RMSD of conductance at 320-380 kHz range. The RMSD values of conductance calculated within 320–380 kHz increase as the amount of strength development increases. Obviously, the RMSD curve measured by PZT sensors and the strength development of concrete have the same trend with the age. This conclusion is well known [29].

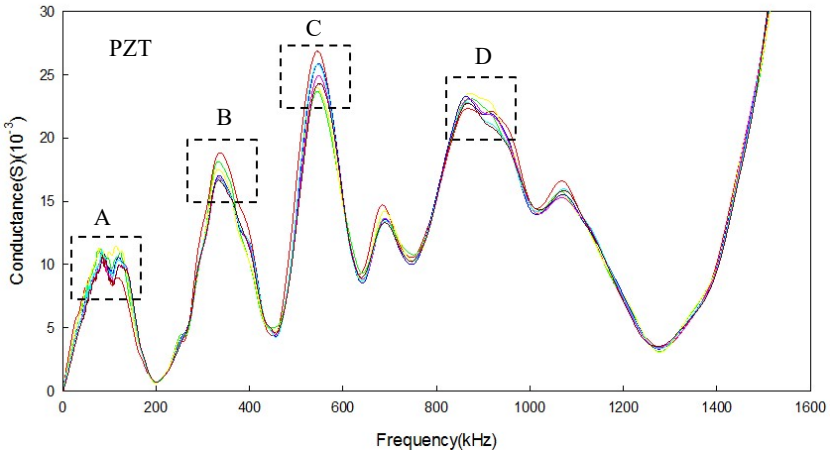

Figure 4. Conductance-frequency curves of the PZT embedded in concrete cylinder at 1–56 days

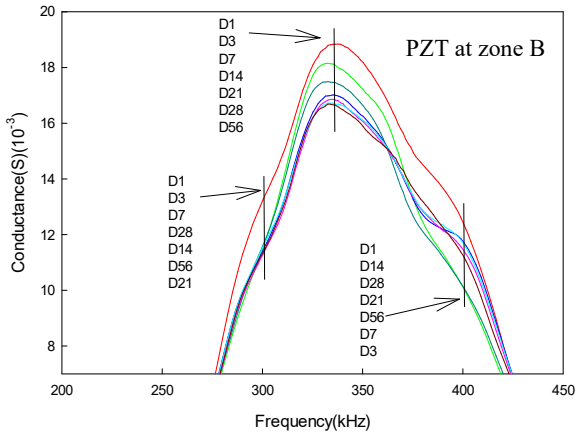

Figure 5. Conductance-frequency curves of the PZT (200–450 kHz).

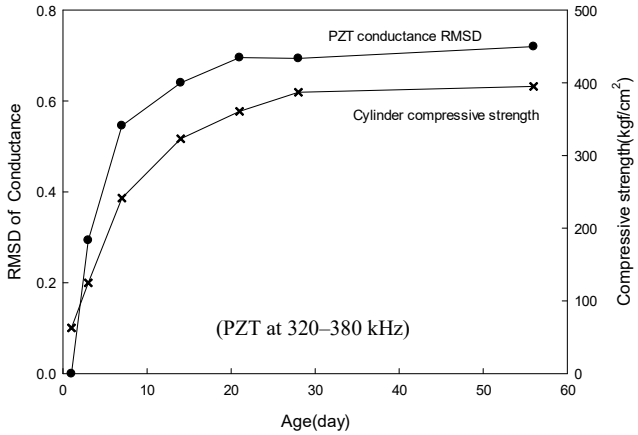

Figure 6. Compressive strength and RMSD of conductance.

For monitoring the strength development by using piezoelectric cement, Fig.7 shows the conductance-frequency curves measured by PPAA and PPBB sensors that embedded in concrete cylinder during 1–56 days. No resonant frequencies are observed for both the PPAA and the PPBB and the conductance-frequency curves are less fluctuated during the age, compared with PZT sensors (Fig. 4). This implies that the span of effective frequency for evaluating conductance variations in sequence by piezoelectric cement sensors is more board than by PZT sensors.

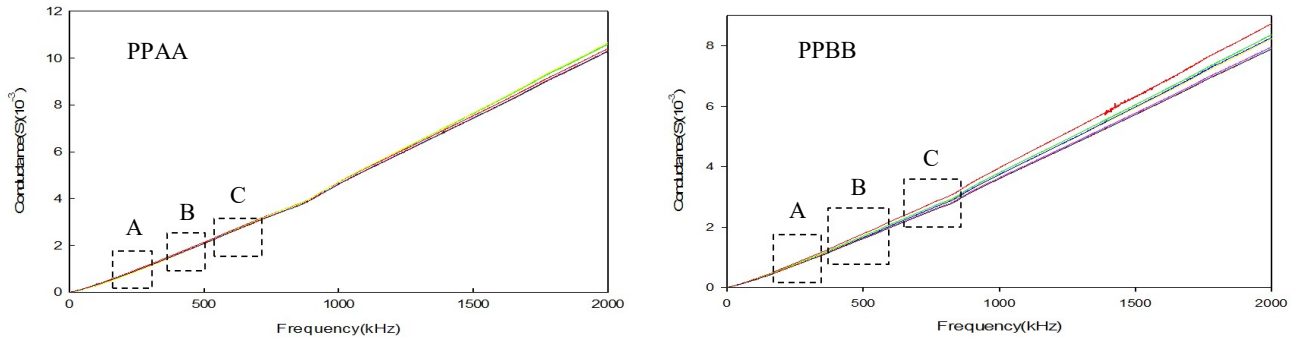

(a) PPAA sensor (b) PPBB sensor

Figure 7. Conductance-frequency curves of (a) the PP and (b) PPBB embedded in concrete cylinder at 1–56 days

After inspect the curves in Fig. 7 which was divided into several zones, for instance zones A, B and C, the range of frequency that reflects the reduction of conductance with increasing the age is anticipated to be located. Fig. 8 (a) is the conductance-frequency curves for the PPAA in zone C (at 600–800 kHz) displayed no conductance reduction in sequence with the age. The only frequency ranges for the PPAA that follow the trend in order is within 500–550 kHz, pretty narrow. However, it is easy to observe such sequences with the age shown in Fig. 8 (b), for instance, in the zone B of the PPBB. The effective frequency ranges satisfying the conductance-age order for the PPBB are within 300–660 kHz.

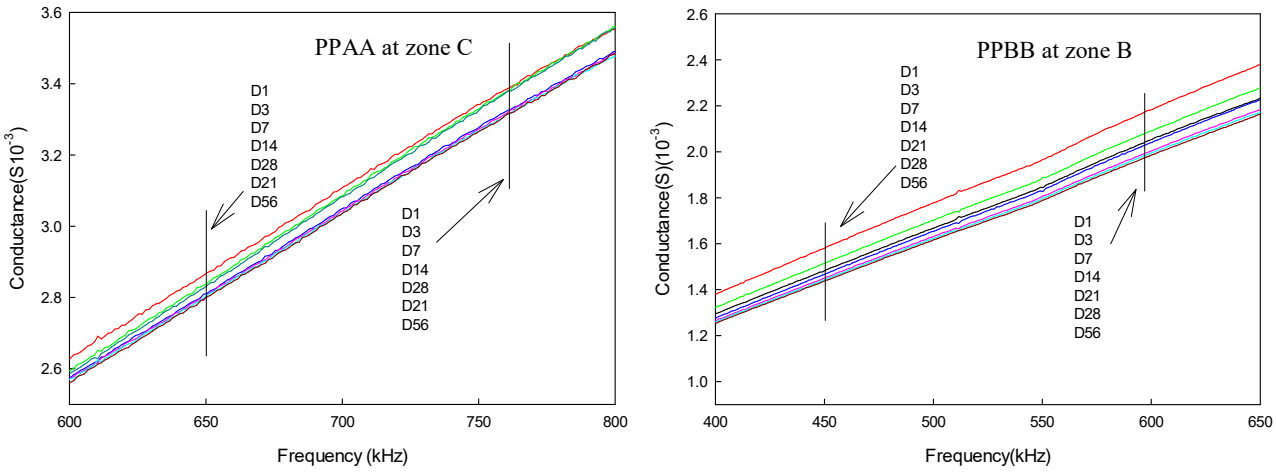

(a) PPAA sensor (600–800 kHz) (b) PPBB sensor (400–650 kHz)

Figure 8. Conductance-frequency curves of (a) the PPAA (600–800 kHz) and (b) the PPBB (400–650 kHz)

The RMSD of conductance was calculated for the PPAA at 500–550 kHz and for the PPBB at 350–650 kHz, depicted in Fig. 9. The RMSD of conductance for both piezoelectric cement sensors can display the strength development with the age. Meanwhile, the behavior of the RMSD curve for the PPBB shown in Fig. 9 (b) more coincide with the strength development than for the PPAA in Fig. 9 (a). This is probably because the PPBB has higher d_{33} than that of the PPAA, shown in Fig. 1.

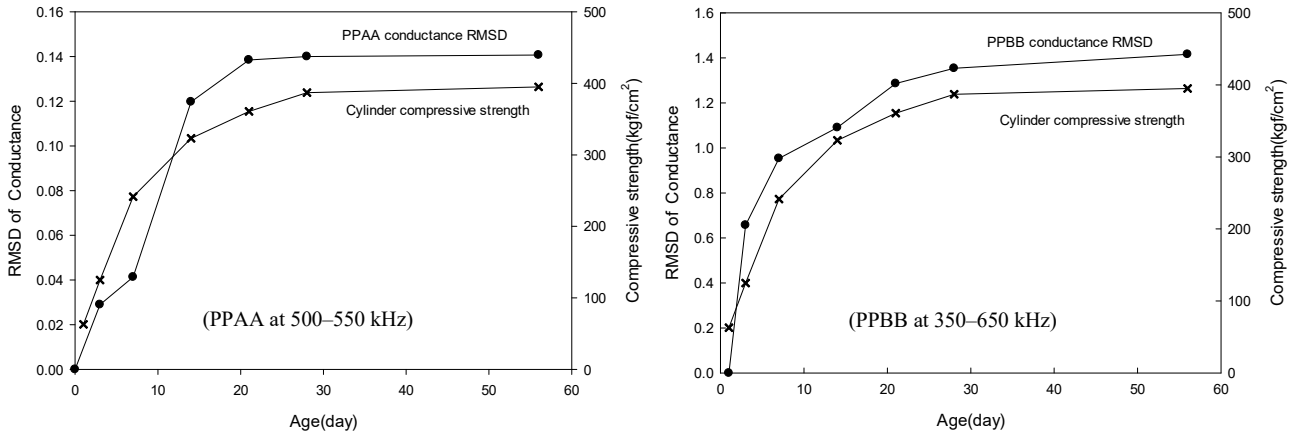

(a) PPAA sensor (500–550 kHz) (b) PPBB sensor (350–650 kHz)

Figure 9. Compressive strength and RMSD of conductance for (a) the PPAA (500–550kHz) and (b) the PPBB (350–650kHz)

3.2 Damage detecting

Three types of piezoelectric sensors (PZT, PPAA and PPBB) were embedded in the concrete beams, respectively. Each beam had four piezoelectric sensors, shown in Fig. 3. Four-point bending test was conducted to the concrete beam at the age of 28 days with applying 0.01 mm/s loading rate. The average fracture load of concrete beam was found with L= 81.8 kN. During the loading, seven loads, 0%L, 20%L, 50%L, 60%L, 70%L, 80%L and 90%L, were chosen to acquire the conductance-frequency spectra of piezoelectric sensors. Fig. 10 shows the crack damage of concrete beam at different loading stages under four-point bending test. More cracks were observed as the loads reach 50%L, and the cracks start to link-up after 50%L.

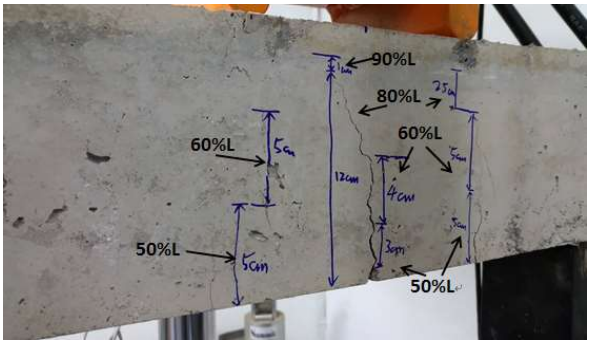

Figure 10. The crack propagation of concrete beam under four-point bending test

For monitoring the conductance-frequency spectra of the PZT sensors embedded in the concrete beam, only resonant frequency peats, especially near the frequency at 360 kHz, were observed having the reduction of conductance consequently as the applied load increases, shown in Fig. 11 for the PZT at position A1 in the interval of 0–200 kHz and 300–400 kHz. One uses the conductance of resonant frequency within 320-380 kHz to plot the conductance-load curves for the PZT at four positions, shown in Fig. 12. The peak values of conductance reduce as the applied load increase, and the conductance reduction is significant after the applied load of 0.5%L. To assess the damage of the concrete beam subjected to external loads, the RMSD of conductance was calculated at the frequency of 340–370kHz and shown in Fig. 13 to investigate the position effect of PZT. Obviously, the position of the embedded sensors near the pre-crack (the middle of the span), i.e., position A1 and B1, has higher RMSD values of conductance than that far away from the main cracks. That means that higher RMSD values for piezoelectric sensor close to the cracks (damage) were found. In addition, the RMSD values have dramatic change after the load of 50%L due to larger crack link-up or propagation. Higher values of RMSD exhibiting more damage of the concrete beam were observed.

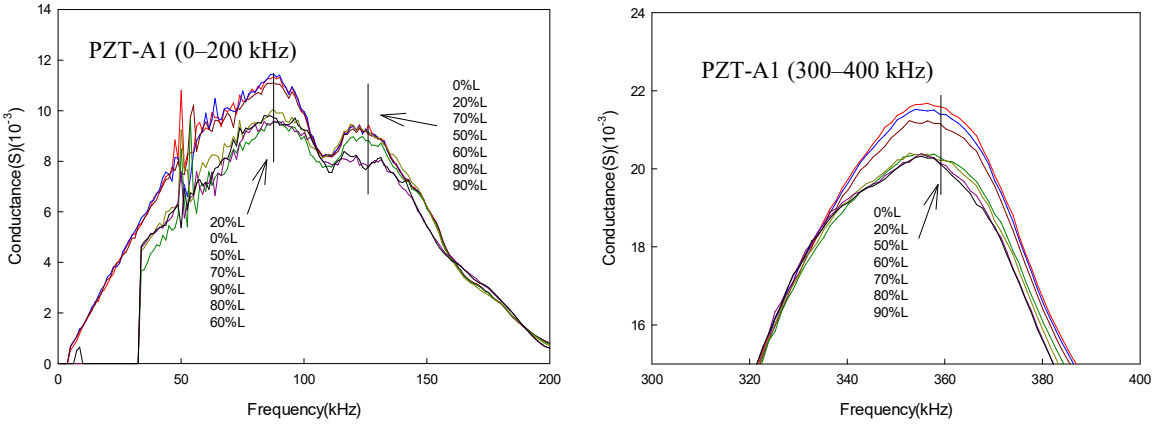

(a) PZT sensor (0–200 kHz) (b) PZT sensor (300–400 kHz)

Figure 11. The conductance of the PZT at A1 position in the interval of (a) 0–200 kHz and (b) 300–400 kHz

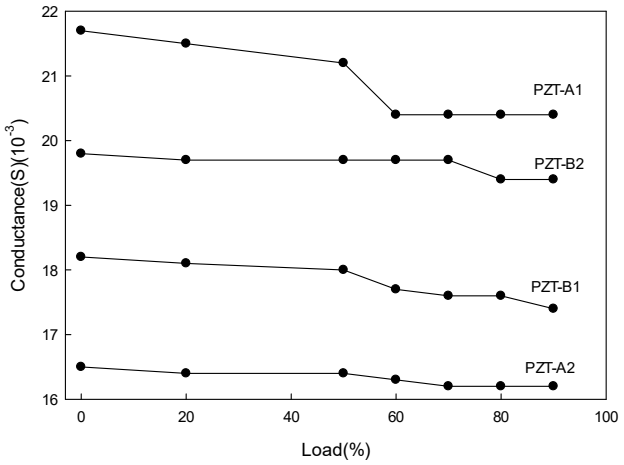

Figure 12. The conductance-applied load relation by the PZT.

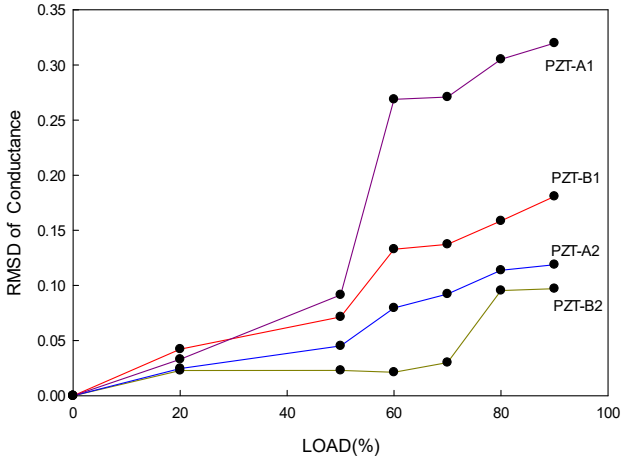

Figure 13. The damage detection by the PZT.

For detecting the damage of the concrete beam by using the piezoelectric cement, Fig. 14 shows the conductance-frequency spectra of the PPBB at position A2, and one finds that the conductance increase as the applied load increases. This observed result is suitable for all PP sensors, but different from the trend that measured by the PZT in Fig. 11. For instance, the relation of conductance and applied load monitored by the PPBB at 1500 kHz is plotted in Fig. 15, and the conductance has an obvious increase, not decrease, after 50%L. The reason for conductance increases with increasing loading measured by piezoelectric cement sensors still needs to be uncovered.

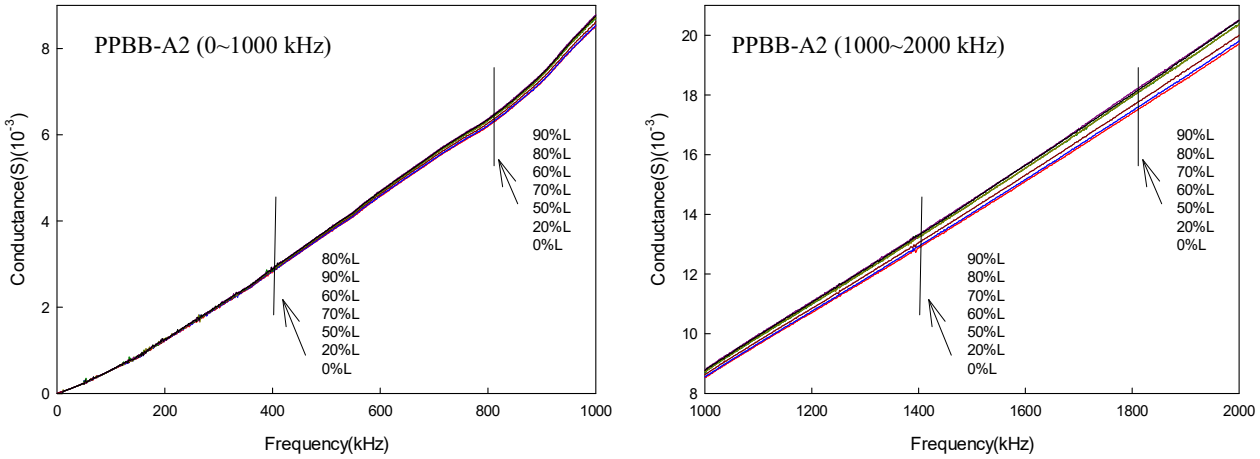

Figure 14. The conductance of the PPBB at A2 position in the interval of (a) 0–1000 kHz and (b) 1000–2000 kHz

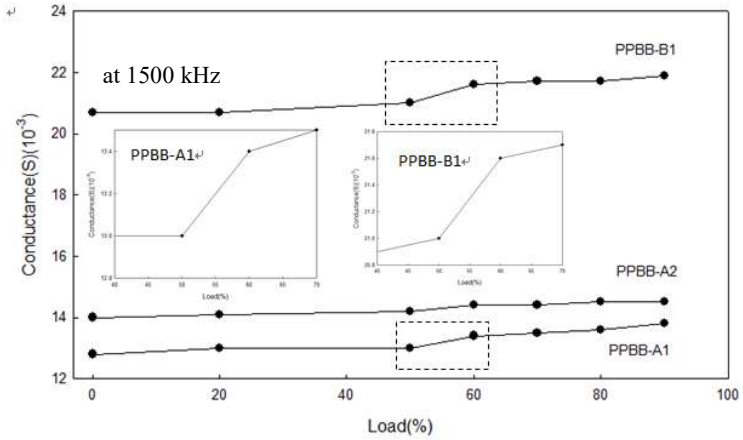

Figure 15. The relation of conductance and applied load monitored by the PPBB at 1500 kHz

The interval of frequency suitable for monitoring the damage of concrete beams by using the PP is within 1000–2000 kHz, shown in Fig. 14. One used the frequency within 1500–1600 kHz to display the RMSD of conductance monitored by the PPAA and PPBB and results are shown in Fig. 16, where the curves for PPAA-A2, PPAA-B1 and PPBB-B2 were not plotted due to the sensors damaged during the loading. The curves of RMSD values of conductance for both the PPAA and the PPBB have a big transition after 50%L, similar to the results shown in Fig. 13 for the PZT, that reflects the damage

of crack propagation of the beam. Hence, one concludes that piezoelectric cement also can be used to detect the crack damage of concrete beam via the EMI technique.

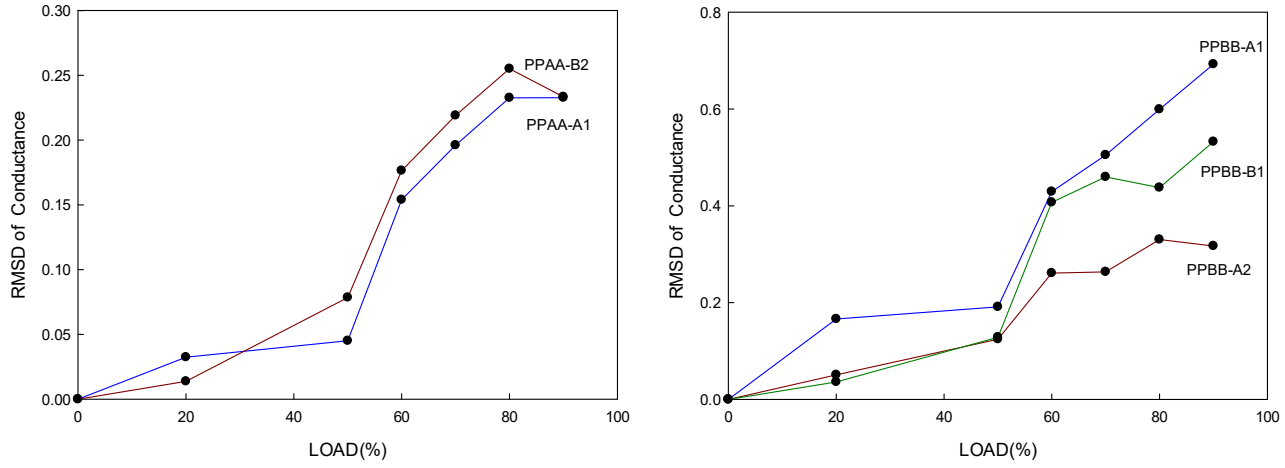

(a) PPAA sensor (b) PPBB sensor

Figure 16. The damage detection by (a) the PPAA and (b) the PPBB in the interval of 1500-1600 kHz

3.3 Comparisons of piezoelectric cement and PZT

Piezoelectric cement sensors embedded in the concrete in conjunction with the electromechanical technique exhibit the ability to monitor the strength development (Fig. 9) and detect the crack damage (Fig. 16) of concrete. For the strength monitoring, the RMSD range of conductance for the PPBB, the PPAA and the PZT approaches to 1.4, 0.14 and 0.7 in turn, shown in Fig. 6 and Fig. 9. This indicates that the RMSD sensitivity of the PPBB is superior to the PPAA and the PZT for the strength development of concrete. Similarly, for the damage detecting the RMSD range of conductance shown in Fig. 13 and Fig. 16 is 0.33, 0.26 and 0.7 approximately for the PZT, the PPAA and the PPBB, respectively. The RMSD sensitivity of the PPBB is still the best, compared with the other two. It seems that piezoelectric cement with higher d_{33} (PPBB) is capable of replacing the PZT for structural health monitoring if the host structure is concrete-made.

4. CONCLUSIONS

The main findings of this phase of research on the use of piezoelectric cement with the EMI technique for the strength monitoring and the damage detecting of concrete are as follows.

- Piezoelectric cement (the PPAA and the PPB) with the EMI technique is capable of monitoring the strength development and the crack damage of concrete structures.
- For structural health monitoring (SHM), the conductance-frequency spectra of piezoelectric cement embedded in concrete showing the characteristic of smooth curves, unlike the PZT having several resonant frequencies, are easy to assess and calculate the conductance variations.

- The effective frequencies of the conductance on the PPBB satisfying the order related to the age of concrete are in the interval of 300–660 kHz, and related to applied loads are 1000–2000 kHz. This board frequency range provides the benefit of larger conductance RMSD.
- Although the capability of SHM by using the PPAA (piezoelectric cement) is worse than that by the PZT sensor, the PPBB (piezoelectric cement) with the piezoelectric strain factor d33 = 101 pC/N is superior to the PZT for SHM.
- Piezoelectric cement with suitable d33 values (the PPBB) has higher sensitivity of conductance RMSD than the PZT for the case of concrete health monitoring.

ACKNOWLEDGEMENTS

This work was financially supported by the Ministry of Science and Technology (Taiwan) under grant number MOST 106-2221-E-992-329.

REFERENCES

[1] Aizawa, S., Kakizawa, T. and Higasino, M., "Case studies of smart materials for civil structures," Smart Mater. Struct., 7, 617-626 (1998).

[2] Soh, C.K., Tseng, K.K.H., Bhalla, S. and Gupta, A., "Performance of smart piezoceramic patches in health monitoring of a RC bridge," Smart Mater. Struct., 9, 533-542 (2000).

[3] Song, G., Gu, H., Mo, Y. L., Hsu, T. T. C. and Dhonde, H. "Concrete structural health monitoring using embedded piezoceramic transducers," Smart Mater. Struct., 16, 959-968 (2007).

[4] Jabir, S. A. A. and Gupta, N. K., "Condition monitoring of the strength and stability of civil structures using thick film ceramic sensors," Measurement, 46, 2223-2231 (2013).

[5] Karthick, S. P., Muralidharan, S., Saraswathy, V. and Thangavel, K., "Long-term relative performance of embedded sensor and surface mounted electrode for corrosion monitoring of steel in concrete structures," Sensors & Actuators B, 192, 303-309 (2014).

[6] Khante, S. N. and Gedam, S. R., "PZT based smart aggregate for unified health monitoring of RC structures," Open J. Civil Eng., 6, 42-49 (2016).

[7] Saraswathy, S., Karthick, S., Lee, H. S., Kwon, S. J. and Yang, H. M., "Comparative study of strength and corrosion resistant properties of plain and blended cement concrete types" Adv. Mater. Sci. Eng., 2017, ID 9454982 (2017).

[8] Panker, B. K. and Khedikar, A. R., "Reinforcement corrosion assessment using PZT sensors via electro mechanical impedance technique," J. Emerging Tech. Innov. Res, 5, 149-152 (2018).

[9] Song, G., Gu, H. and Mo, Y. L., "Smart aggregates: multi-functional sensors for concrete structures—a tutorial and a review," Smart Mater. Struct., 17 (3), 033001 (2008).

[10] Xu, D., Cheng, X., Huang, S. and Jiang, M., "Electromechanical properties of 2-2 cement based piezoelectric composite," Curr. Appl. Phys., 9, 816-819 (2009).

[11] Zhang, J., Lu, Y., Lu, Z., Liu, C., Sun, G. and Li, Z., "A new smart traffic monitoring method using embedded cement-based piezoelectric sensors", Smart Mater. Struct., 24, ID 025023 (2015).

[12] Xu, D., Huang, S. and Cheng, X., "Electromechanical impedance spectra investigation of impedance-based PZT and cement/polymer based piezoelectric composite sensors", Constr. Build. Mater., 65, 543-550 (2014).

[13] Li, Z. J., Zhang, D. and Wu, K. R., "Cement-based 0-3 piezoelectric composites," J. Am. Ceram. Soc., 85, 305-313 (2002).

[14] Cheng, X., Huang, S., Chang, J., Xu, R., Liu, F. and Lu, L., "Piezoelectric and dielectric properties of piezoelectric ceramic–sulphoaluminate cement composites," J. Euro. Ceram. Soc., 25, 3223-3228 (2005).

[15] Huang, S., Chang, J., Lu, L., Liu, F., Ye, Z. and Cheng, X., "Preparation and polarization of 0–3 cement based piezoelectric composites," Mater. Res. Bull., 41, 291-297 (2006).

[16] Chaipanich, A., Jaitanong, N. and Tunkasiri, T., "Fabrication and properties of PZT–ordinary portland cement composites,", Mater. Lett., 61, 5206-5208 (2007).

[17] Gong, H., Zhang, Y., Quan, J. and Che, S., "Preparation and properties of cement based piezoelectric composites modified by CNTs," Curr. Appl. Phys., 11, 653-656 (2011).

[18] Wang, F., Wang, H., Song, Y. and Sun, H., "High piezoelectricity 0-3 cement-based piezoelectric composites," Mater. Lett., 76, 208-210 (2012).

[19] Pan, H. H., Yang, R.H. and Cheng, Y. C., "High piezoelectric properties of cement piezoelectric composites containing kaolin," Proc. SPIE, 9437, 94370R (9 pp.) (2015).

[20] Pan, H. H., Lin, D. H. and Yang, R. H., "High Piezoelectric and dielectric properties of 0-3 PZT/cement composites by temperature treatment," Cem. Conc. Compos., 72, 1-8 (2016).

[21] Dong, B., Xing, F. and Li, Z. J., "Electrical response of cement-based piezoelectric ceramic composites under mechanical loadings," Smart Mater. Res., 2011, ID 236719 (2011).

[22] Wang, F. Z., Wang, H., Sun, H. J. and Hu, S. G., "Research on a 0–3 cement-based piezoelectric sensor with excellent mechanical–electrical response and good durability," Smart Mater. Struct. 23, 045032 (7pp.) (2014)

[23] Qin, L., Lu, Y. and Li, Z., "Embedded Cement-Based Piezoelectric Sensors for Acoustic Emission Detection in Concrete," J. Mater. Civ. Eng., 22, 1323-1327 (2010).

[24] Lu, Y. and Li, Z., "Frequency characteristic analysis on acoustic emission of mortar using cement-based piezoelectric sensors," Smart Struct. Sys., 8, 321-341 (2011).

[25] Lu, Y., Zhang, J., Li, Z. and Dong, B., "Corrosion monitoring of reinforced concrete beam using embedded cement-based piezoelectric sensor," Mag. Conc. Res., 65, 1265-1276 (2013).

[26] Zhou, H., Liu, Y., Lu, Y., Dong, P., Guo, B., Ding, W., Xing, F., Liu, T. and Dong, B., "In-situ crack propagation monitoring in mortar embedded with cement-based piezoelectric ceramic sensors," Constr. Build. Mater., 126, 361-368 (2016).

[27] Liang, C., Sun, F. P. and Rogers, C. A., “Coupled electromechanical analysis of adaptive material systems – determination of the actuator power consumption and system energy transfer,” J. Intel. Mater. Sys. Struct., 5, 12-20 (1994).

[28] Pan, H. H., Wang, C. K. and Cheng, Y. C., “Curing time and heating conditions for piezoelectric properties of cement-based composites containing PZT,” Constr. Build. Mater., 129, 140-147 (2016).

[29] Shin, S. W. and Oh, T. K., “Application of electric-mechanical impedance sensing technique for online monitoring of strength development in concrete using smart PZT patches,” Constr. Build. Mater.,23, 1185-1188 (2009).

[30] Park, G., Sohn, H., Farrar, C. R. and Inman, D. J, “Overview of piezoelectric impedance-based health monitoring and path forward,” Shock Vib. Dig., 35, 451-463 (2003).